Rev. Roum. Sci. Techn.– Électrotechn. et Énerg.
Vol. **70**, *1*, pp. 15–20, Bucarest, 2025

PARTICULARITIES OF ROTOR FIELD ORIENTATION CONTROL IMPLEMENTATION ON INDUSTRIAL DSP SYSTEMS

CONSTANTIN VLAD SURU[1], ALEXANDRU BITOLEANU[2], MIHAELA POPESCU[3], MIHAITA LINCA[4], FLORIN RAVIGAN[5]

Keywords: Digital signal processing (DSP) control; Traction system; Rotor field orientation; Induction motor.

The aim of this paper is the experimental implementation and validation of field-oriented control for asynchronous machine traction systems, on the one hand, with a special interest in the motor flux estimator and the implementation intricacies specific to the DSP implementation of discrete control systems, on the other hand. The implementation was done on a prototyping dSPACE DS1103 control system for an experimental 50 kW induction motor experimental stand. The prototyping system programming was done in the MATLAB/Simulink environment. Given that the control algorithm is intended to be used in an industrial system, the control model must be suitable to be converted into production code. Therefore, the study aims to overcome the limitations of industrial DSP systems for rotor field-oriented drive systems with induction motors.

1. INTRODUCTION

The traction systems with induction motors have some properties typical of ordinary drive systems, such as high power and the ability to function at the traction motor's rated speed. Above the motor-rated speed, the developed electromagnetic torque is diminished, given the motor's maximum power; therefore, the traction system mechanical load is low, but the vehicle can reach high running speed. At the same time, the motor flux must be diminished to avoid the motor saturation. This leads to a demanding regime for the traction motor and a specific demanding regime for the control system.

This is because the rotor field orientation control can only be physically implemented on high computation power DSP systems, given the complexity of the control algorithm to be executed in real-time and the acquisition of several instantaneous electrical signals [1].

From the control algorithm, some computations are sensitive to computing errors, such as the motor flux estimator. Suppose the computing errors are high due to the limitation of the adopted computing method. In that case, the estimated flux deviates from the actual value, and the control system has difficulties regulating quantities that do not follow reality.

It was observed that the estimated flux tends to increase because of computing errors. Consequently, the flux controller, whose output is the d-axis current, reduces its output to regulate the flux. Because the higher the speeds, the higher the errors, for a given time step, at some speed value, the flux controller output reaches the lower limit, it saturates, and the system loses the orientation.

This paper analyzes the flux estimation applicable to real-time implementation. The flux estimator was implemented within the rotor field orientation control algorithm for a dSPACE DS1103 prototyping board in the Matlab Simulink environment. The control system was applied to a 50 kW experimental traction stand. The purpose of the study is to export the algorithm to an industrial application (railway vehicle).

2. ROTOR FIELD ORIENTED CONTROL

Field orientation control is a suitable control method for drive systems with induction motors and voltage inverters designed for traction applications [2–6]. In addition to the necessary control loops, an important matter is estimating the motor flux from the available measurable quantities [3–5].

The literature contains different techniques, and among the methods investigated by the authors [4], the motor flux estimation based on the stator currents and rotor speed was considered for implementation on a scale experimental electric traction stand and is considered "transducer friendly."

The field-oriented control inputs are the imposed motor current projections on the d-q referential (synchronized to the rotor), which is the magnetizing current on the d-axis and the active current on the q-axis. Two controllers impose the motor currents: i_d is given by the motor flux controller, and i_q is typically imposed by the speed controller.

For the computation of the actual motor current projection on the d-q axes, the rotor angle (λ) is necessary. The rotor angle is obtained from the rotor flux, considering its magnitude and projections, on the α and β axes [4][6]:

$$\Psi_r = \sqrt{\Psi_{r\alpha}^2 + \Psi_{r\beta}^2}, \tag{1}$$

$$\cos\lambda = \frac{\Psi_{r\alpha}}{\Psi_r}; \sin\lambda = \frac{\Psi_{r\beta}}{\Psi_r}, \tag{2}$$

where the rotor flux projection is [1,4]:

$$\Psi_{r\alpha} = \int \left(-p\omega\Psi_{r\beta} - \frac{R_r}{L_r}\Psi_{r\alpha} + \frac{L_m \cdot R_r}{L_r} i_{s\alpha}\right) \mathrm{d}t, \tag{3}$$

$$\Psi_{r\beta} = \int \left(p\omega\Psi_{r\alpha} - \frac{R_r}{L_r}\Psi_{r\beta} + \frac{L_m \cdot R_r}{L_r} i_{s\beta}\right) \mathrm{d}t. \tag{4}$$

Figure 1 illustrates the control algorithm. The Clarke and Park transformations obtained the motor current projections on the d-q referential (attached to the rotor). The three-phase imposed currents were also obtained using reverse Park and reverse Clarke transformations.

The flux estimator requires the integral of the α–β projections of the motor flux, whose numeric implementation is essential in real-time applications.

3. PAPER TITLE

The Euler integration method is implemented using the sample recurrence [7–9]:

$$y_{k+1} = y_k + T_s \cdot f(t_k, y_k) \tag{5}$$

where:

- y_k - current sample;
- t_k - current sample time;

[1] University of Craiova, Faculty of Electrical Engineering, Decebal Blvd., no 107, Craiova, Romania.
E-mails: vsuru@em.ucv.ro, alex.bitoleanu@em.ucv.ro, mpopescu@em.ucv.ro, mlinca@em.ucv.ro, [f]lorin.ravigan@ie.ucv.ro

DOI: 10.59277/RRST-EE.2025.1.3

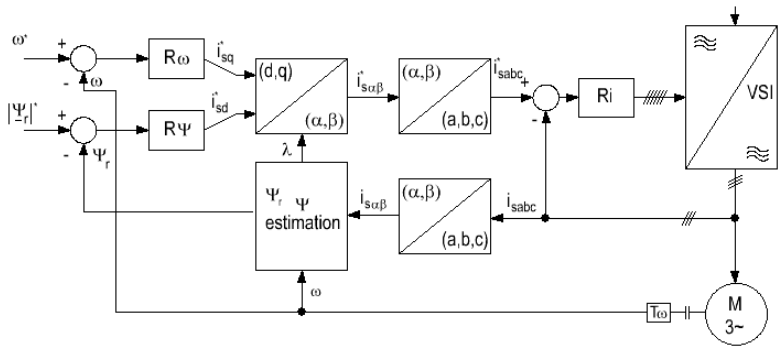

Fig. 1 – Control algorithm for flux estimation based on motor currents and rotor speed.

- y_{k+1} next computed sample;
- T_s sample period;
- $f(t_k, y_k)$ the variable derivative estimation function.

The estimation function of the variable derivative uses the rectangle method; therefore, the computation error is higher at relatively high sample periods [7,8].

4. HEUN INTEGRATION IMPLEMENTATION

The computation error is high when using the Euler integration method in the flux estimator, leading to the drive system's inability to reach the maximum speed range.

At the same time, because the field-oriented control algorithm is intended to run on an industrial DSP, which cannot work at sample times below 40 μs, the field estimator integrator computation error must be reduced. The way to do this is by implementing a higher-order integration method, and the first method to start with is the second-order integration method, the Heun method.

To reduce the computation error, the Heun method uses the trapezoidal method to estimate the integral [7,9–10]:

$$y_{k+1} = y_k + \frac{T_s}{2}[f(t_k, y_k) + f(t_{k+1}, y_{k+1})]. \quad (6)$$

The disadvantage of this method is the fact that the derivative at the next step ($f(t_{k+1}, y_{k+1})$) is not yet known. Therefore, it is estimated based on the Euler method [7,9–10]:

$$y^*_{k+1} = y_k + T_s f(t_k, y_k). \quad (7)$$

This approximation is later used in (10) [7,9–10]:

$$y_{k+1} = y_k + \frac{T_s}{2} \cdot [f(t_k, y_k) + f(t_{k+1}, y^*_{k+1})]. \quad (8)$$

5. FIELD ORIENTED CONTROL IMPLEMENTATION FOR DS1103 PROTOTYPING BOARD

The presented method for estimating the rotor flux had been implemented for an experimental drive system stand corresponding to a scaled-size electric locomotive traction system. The rated parameters of the stand traction motor are:

- U_N = 380 V; $_N$ = 88 A; P_N = 50 kW;
- f_N = 65 Hz; n_N = 1917 rpm.

The traction motor mechanical load is a DC machine used as a DC generator with a fixed resistive load, so the resistive torque is obtained by tuning the field current.

The three-phase traction inverter is built with high-power IGBTs corresponding to the full-size locomotive traction system (PN = 1.5 MVA). The inverter is fed from a single-phase PWM boost rectifier, allowing the system to recover the braking power back to the power grid. The DC-Link voltage is 700 V. Given the high power IGBTs used, the switching frequency (imposed to the PWM modulators) is 1 kHz, although the power is low.

A dSPACE DS1103 prototyping board controls the inverter. This gives the advantage of implementing the control algorithm of the drive system in the MATLAB/Simulink environment as a Simulink model (Fig. 2). The model is grouped into several subsystems:

- *Motor current and flux computation* – this block includes the flux estimator and the Clarke and Park transformations for the motor current and flux;
- *Rotor flux control* – the rotor flux control loop with proportional integrative controller;
- *D-axis and q-axis current controllers* – proportional integrative controllers;
- *Magnetizing current* – block for estimation of the magnetizing current, given the magnetizing inductance, the motor current on the d-q referential and imposed flux;
- *Transf_R-S* – reverse Park and reverse Clarke transformations;
- *Speed controller* – proportional integrative speed controller with variable saturation limits;
- *Torque2isq* – block for conversion of the torque limit to q-axis current limit, applied to the speed controller.
- Simulink blocks from dSPACE Real-Time Interface Library – blocks that represent the links between the Simulink signals and the DS1103 hardware resources (PWM modulator, analog to digital converters, *etc*.) [11];
- General Simulink blocks are needed for the experimental system's real-time control (imposed values of speed and torque, validation signals, *etc*.).

The flux estimator model for the Euler integration method is illustrated in Fig. 3, where it can be observed that it uses the standard Simulink integrator block. Also, the direct implementation of (3) and (4) was done. The solver implements the numerical integration method – Ode1 (Euler) [12].

The flux estimator model for the Heun integrators is illustrated in Fig. 4. An important fact is that only the integrators in the flux estimator must be 2nd order (Heun). The other integrators in the control model (the flux controller, the d and q current controller, and the speed controller) do not need special requirements and can be 1st order (Euler).

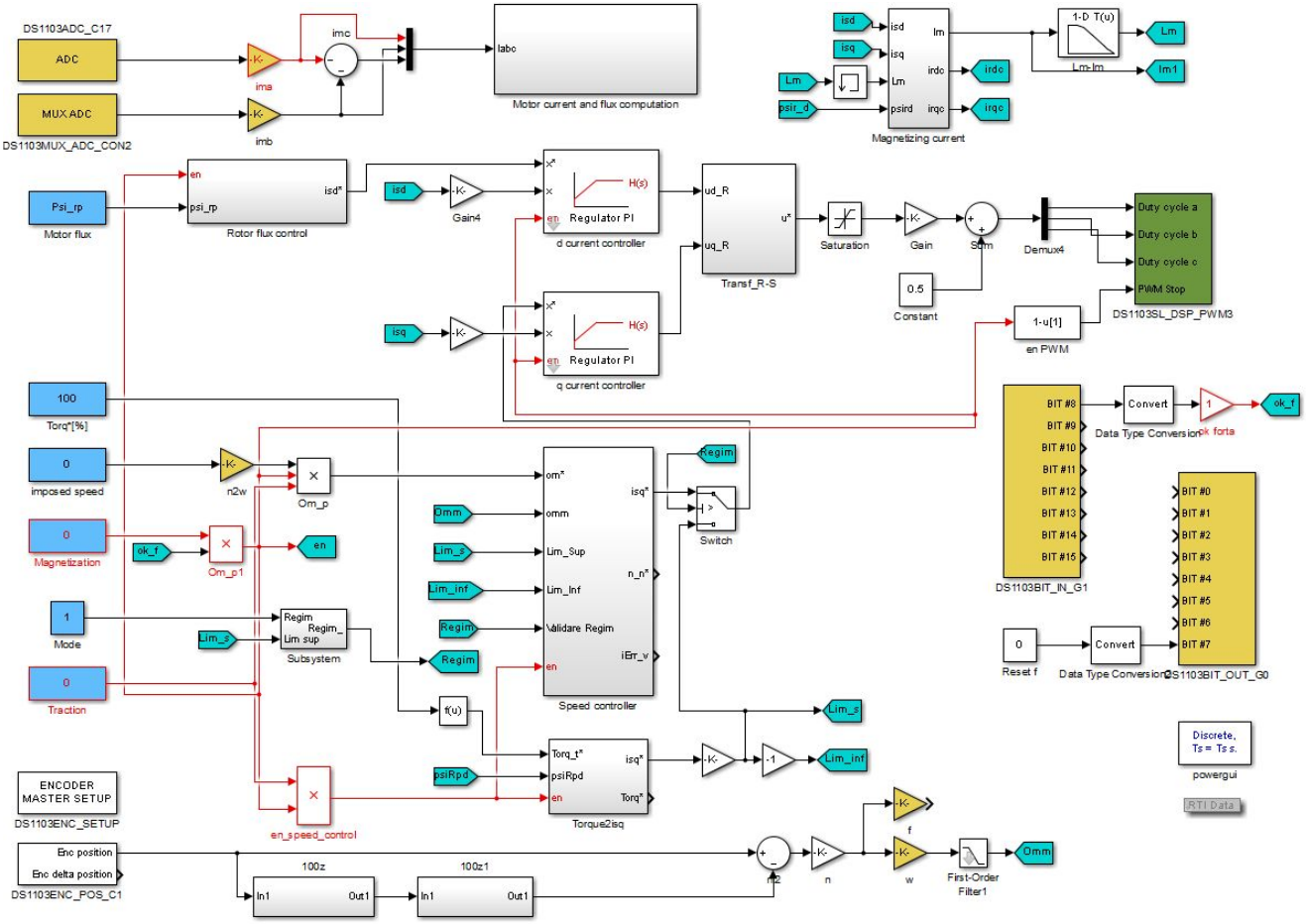

Fig. 2 – Experimental drive system control model for dSPACE DS1103 prototyping board.

Of course, they can be implemented as 2nd order integrators, but the Simulink control model for the DS1103 is intended to be transformed into C production code for an industrial DSP. Therefore, second-order integrators require more computing power, on the one hand, and the production code is obtained by TargetLink, on the other hand, so the numerical implementation of second-order integrators cannot be implemented by the Simulink solver [12,13]. Consequently, the flux estimator using 2nd order integration was implemented based on (7) and (8), not using the Simulink integrator block – Fig. 4.

The motor flux estimator needs the acquisition of the motor currents and the rotor speed, which are available to the dSPACE board from the power inverter output current transducers and the motor shaft incremental encoder, respectively. The current transducer outputs applied to the DS1103 analog inputs are available to the control model as Simulink signals (given by the DS1103ADC blocks and scaled according to the range of the current transducer and the DS1103 board input range [11]).

The speed is obtained from an incremental encoder mounted inside the motor case. As the encoder input block (DS1103ENC_POS_C1) gives the current position index, the transformation to speed was necessary. As seen in Fig. 2, a sliding window filter was implemented to reduce the speed ripple due to the limited number of impulses per revolution (giving a mediation of 8 ms). A 200 Hz low pass filter further filtered the speed. The speed controller is a special proportional-integrative controller (its output (*i.e.*, q-axis current) is dynamically limited to limit the motor-generated torque).

The d- and q- axes current controllers are proportional-integrative controllers with their outputs applied to the DS1103 board PWM modulators (after the corresponding transformations form d-q to abc referential).

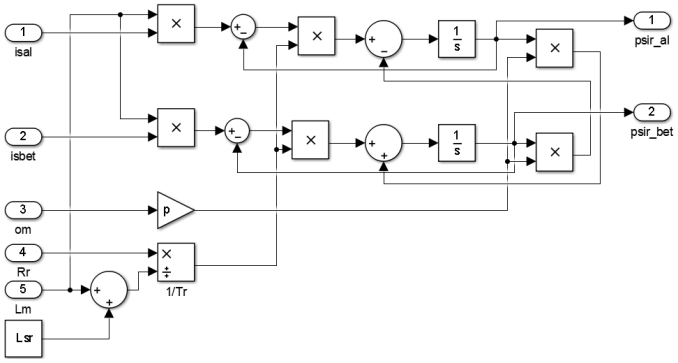

Fig. 3 – The flux estimator for Euler integrators.

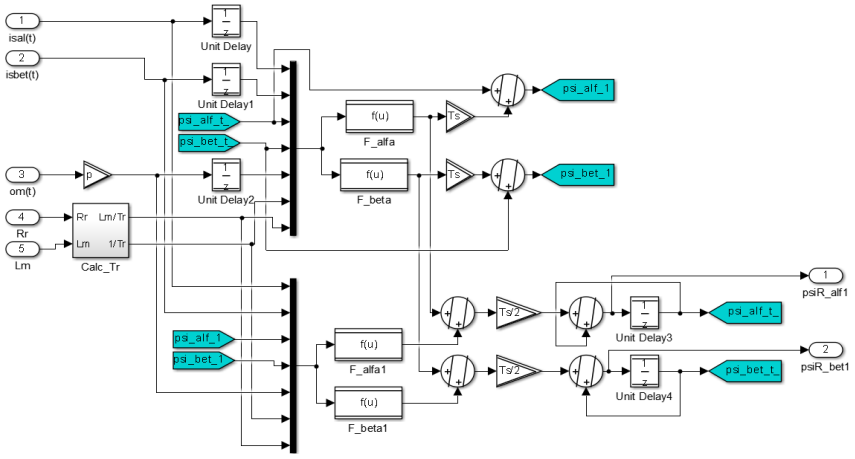

Fig. 4 – The flux estimator for the Heun integration method.

The sample time was chosen to 40 µs. This value was imposed by the fact that the control algorithm must be executable in real-time by industrial DSP systems with fewer hardware resources than the DS1103 board.

The Simulink ODE solver method used to compute the model states for model simulation is also used for DSP real-time integrators. The more complex the solver, the more time it needs for the computations, so the solver must be chosen as simply as possible [12]. Ode1 solver was selected for the model in Fig. 2 because for the conversion of the control model to production code (with TargetLink), for industrial DSP, only the Euler integration method can be used for the implementation of integrators [13].

A virtual control panel built into the dSPACE application software, ControlDesk NG (Fig. 5), assures real-time control of the experimental system [14]. The virtual instruments are linked to the Simulink control model block parameters and signals; therefore, the signals can be read or controlled using the block parameters [14–16]. It must be noted that the analog meters do not perform any measurement but display a Simulink signal value.

6. EXPERIMENTAL RESULTS

The drive system was tested by imposing the motor-rated and twice-rated speeds. To limit the power dissipation of the DC generator resistive load (at higher speeds) and not exceed the DC generator rated power (above the traction motor rated speed), the field generator current was 5A at first and later reduced to 3A. Above the rated speed, the field current was decreased again to 1.5A.

A) EULER INTEGRATION METHOD

The speed control loop was validated after the motor was magnetized, and the imposed speed linearly increased to the rated speed of 1500 rpm – Fig. 6.

The measured speed increases towards the imposed speed with little error when the electromagnetic torque is below the 80% limit (Fig. 5), and slower after the torque limit is reached (Fig. 5, Fig. 6). When the generator field current is reduced to 3A, the speed rapidly reaches the imposed value. Finally, the speed is reduced to zero by regenerative braking (i_q has a negative component – Fig. 7). The results show that the traction system works well.

An important conclusion relevant to this study is drawn from the motor-calculated flux and the corresponding current on the d-axis (Fig. 8, Fig. 9). Although the motor flux is well regulated, the d-axis current necessary to obtain this flux is not constant.

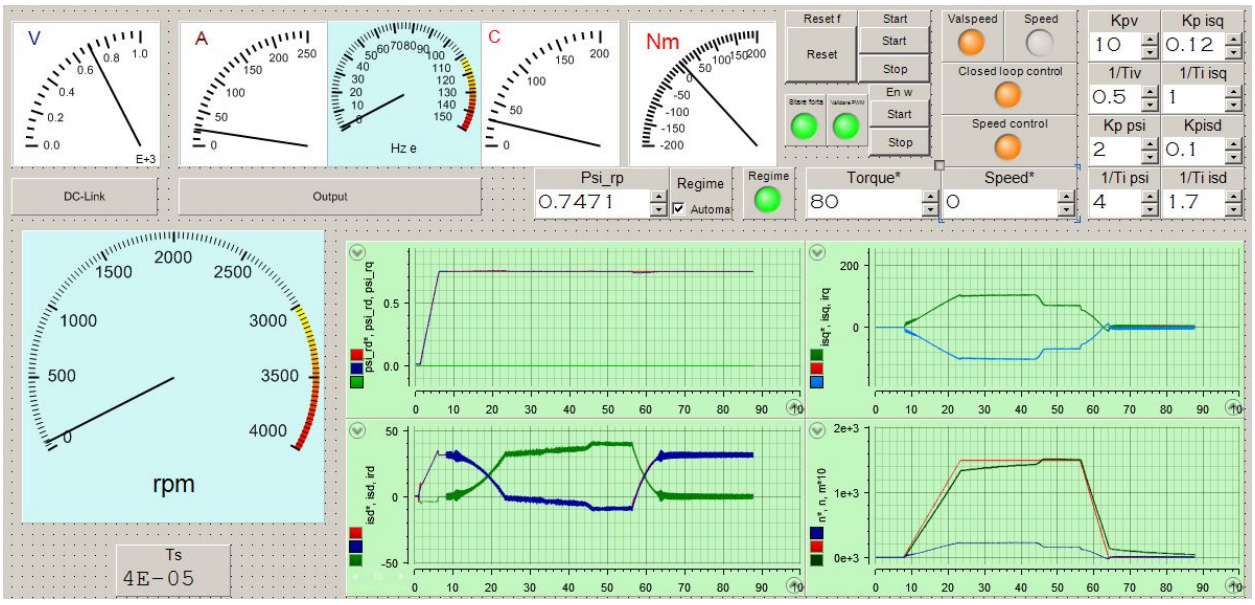

Fig. 5 – ControlDesk NG virtual control panel of the experimental drive system for the Euler integrator in the flux estimator.

Precisely, to maintain the flux to the imposed value, the d-axis current decreases as the speed increases.

The d-axis current is also dependent on the load. Still, in a lower proportion: for the imposed speed of 1500 rpm, the necessary d-axis current to maintain the flux at 0.74 Wb is -8.69 A, for the 3A generator field current, and -7.49A at no load operation. This peculiar effect is given by the computing errors produced by the ode1 integrators in the motor flux estimator. Therefore, the estimated flux tends to increase as the speed increases, so the d-axis current is adjusted to regulate the flux.

The same experiment, for 20 μs time sample, is detailed in Fig. 10. The current evolution is slightly different because the generator field current was set directly at 3A. Still, the critical fact is that the imposed d-axis current necessary to regulate the motor flux decreases less, compared to the 40 μs time step, and does not become negative (13.16 A).

This means that the d-axis current does not follow the mathematical model and the physical phenomenon because, although the motor flux is constant, the d-axis current is not.

The maximum speed that can be reached for a given time sample depends on the necessary current value to keep the motor flux at its imposed value. The system loses orientation when the flux controller output (d-axis current) reaches the lower limit of 61.2 A.

B) HEUN INTEGRATION METHOD

In the first place, it can be observed that the motor speed could be increased up to about 150% of the nominal value (2800 rpm). The motor speed could not be increased over 3000 rpm because the DC generator's maximum speed would be exceeded. Also, the generator field current was reduced to 2 A so as not to exceed the rated power of the machine.

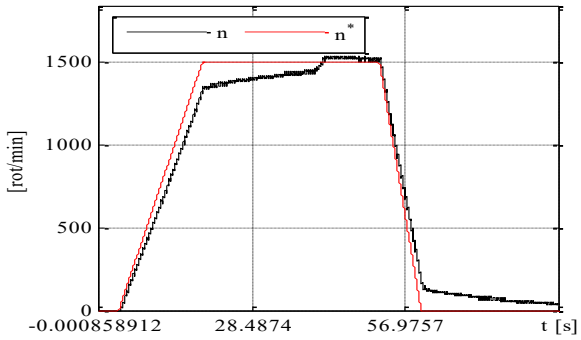

Fig. 6 – The motor speed for the Euler integration method in the flux estimator.

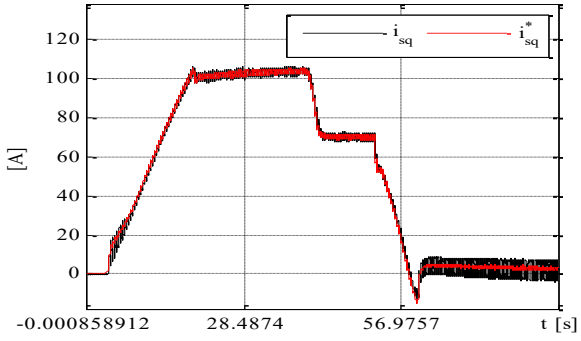

Fig. 7 – The q-axis traction motor current for the Euler integration method in the flux estimator.

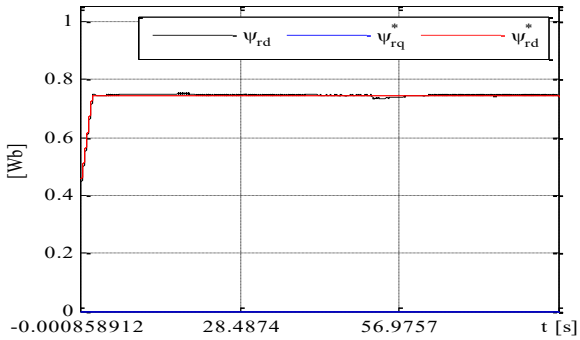

Fig. 8 – The motor calculated flux for the Euler integration method in the flux estimator.

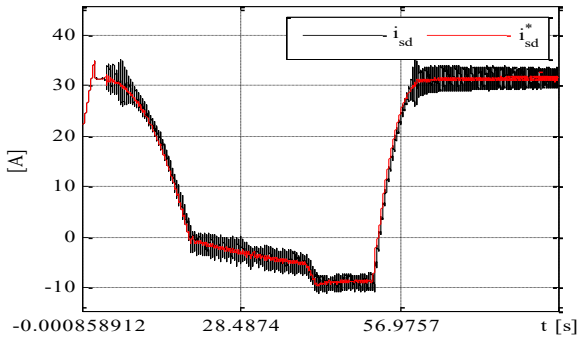

Fig. 9 – The motor current on d-axis for a 40 μ time step for the Euler integration method in the flux estimator.

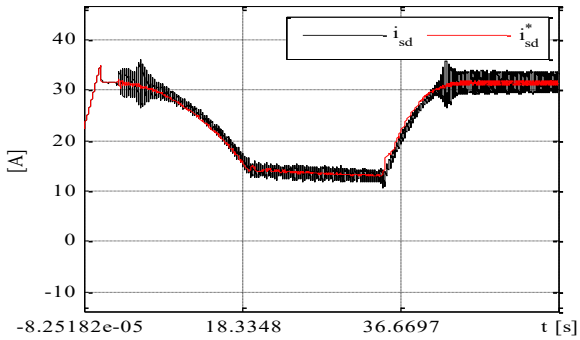

Fig. 10 – The traction motor d-axis current for a 20 μs time step for the Euler integration method in the flux estimator

The estimated motor flux is illustrated in Fig. 13. The flux regulation is better than the Euler-based flux estimator. At the same time, for the same sample time (40μs) and control system parameters, the real currents on the dq axes have a higher ripple, although the regulation is better. For this case, the evolution of the d-axis current is in accord with the rotoric flux.

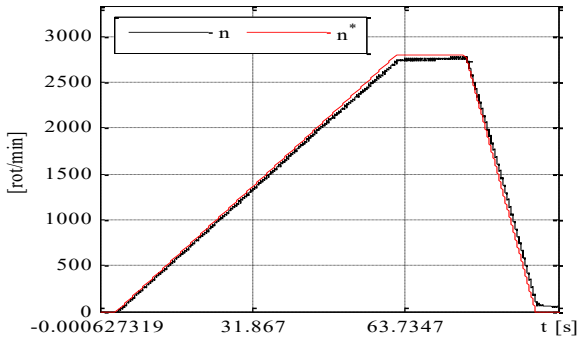

Fig. 11 – The traction motor speed for the Heun integration method in the flux estimator.

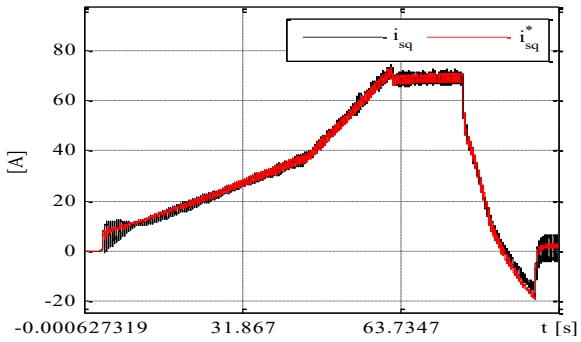

Fig. 12 – The q-axis traction motor current for the Heun integration method in the flux estimator.

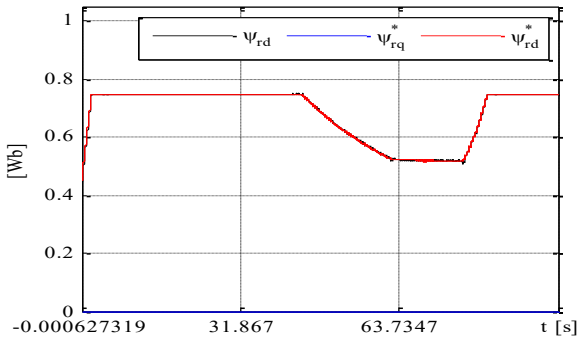

Fig. 13 – The motor calculated flux for the Heun integration method in the flux estimator.

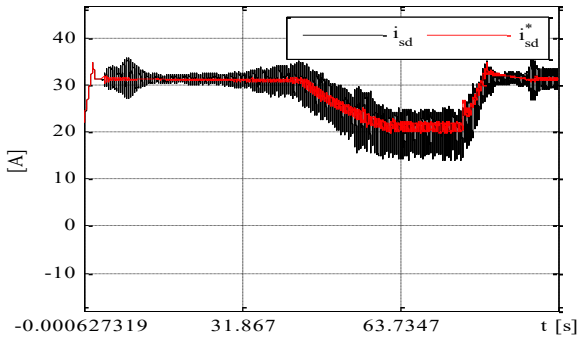

Fig. 14 – The flux estimator's d-axis current for the Heun integration method.

Thus, the d-axis current is constant when the flux is constant and decreases when the traction motor-rated speed is above the nominal value because the flux is diminished, as confirmed in Fig. 13.

7. CONCLUSIONS

Some difficulties were encountered in implementing a rotor field orientation control system for an induction motor traction system. These consisted of the impossibility of driving the motor above the rated speed because the d-axis current imposed to control the motor flux lowers as the speed increases until the flux controller's lower output limit is reached, and the system loses orientation. This limitation is due to the computation errors in the flux estimator. This is because the flux estimator uses two integrators, which are numerically implemented using the Euler integration method, which is known to lead to high computation errors at high computation time steps. A theoretical solution to this problem is reducing the computation time step. Still, this solution cannot be adopted as industrial DSP systems used for real-time control cannot handle the necessary low sample time. The solution to this problem, which was implemented and experimentally validated, consists of using the second-order Heun integration method in the flux estimator. It has been proven that the computation errors are low enough for the system to function correctly. Consequently, the d-axis current value is dependent only on the rotor flux.

CREDIT AUTHORSHIP CONTRIBUTION STATEMENT

Constantin Vlad Suru: 35%
Alexandru Bitoleanu: 20%
Mihaela Popescu: 20%
Mihaita Linca: 15%
Florin Ravigan: 10%

Received on 14 November 2024

REFERENCES

1. A. Bitoleanu, M. Popescu, C.V. Suru. *Implementation of rotor flux-oriented control on traction system of autonomous electric locomotives*, International Conference on Electromechanical and Energy Systems (SIELMEN), 1-6 (2023).
2. S. Benaicha, *Robust sensorless speed control of an induction motor drive using a synergetic approach*, Rev. Roum. Sci. Techn. – Électrotechn. Et Énerg, **68**, *4*, pp. 381–387 (2023).
3. A. Ahriche, M. Kidouche, A. Idir, Y. Deia, *Combining sliding mode and second Lyapunov function for flux estimation*, Rev. Roum. Sci. Techn. – Électrotechn. Et Énerg, **61**, *2*, pp. 106-110 (2016).
4. M. Popescu, A. Bitoleanu, C.V. Suru, *Estimation of the rotor flux in the traction systems with induction motors and field-oriented control*, International Conference on Electromechanical and Energy Systems (SIELMEN), Craiova, Romania, pp. 1-6 (2023).
5. R. Bojoi, G. Griva, F. Profumo, *Field-oriented control of dual three-phase induction motor drives using a Luenberger flux observer*, IEEE Industry Applications Conference Forty-First IAS Annual Meeting, Tampa, FL, USA, pp. 1253-1260 (2006).
6. X. Xu, D.W. Novotny, *Implementation of direct stator flux orientation control on a versatile DSP based system*, IEEE Industry Applications Society Annual Meeting, **1**, pp. 404-409 (1990).
7. U.M. Ascher, L.R. Petzold, *Computer Methods for Ordinary Differential Equations and Differential-Algebraic Equations*. Philadelphia: Society for Industrial and Applied Mathematics (1998).
8. J.C. Butcher, *Numerical Methods for Ordinary Differential Equations*, New York, John Wiley & Sons (2003)
9. A. Hadăr, C. Marin, C. Petre, A. Voicu, *Numerical Methods in Engineering* (in Romanian), Politehnica Press, București (2004).
10. C.F. Chan Man Fong, D.D. Kee, P.N. Kaloni, *Advanced Mathematics for Engineering and Science*, MA, USA: World Scientific (2003).
11. *** Real-Time Interface (RTI and RTI-MP) Implementation Guide, release 5.2, dSpace Gmbh (2006).
12. ***Simulink Solvers – Simulink, https: //www.mathworks.com/ help/ simulink/gui/solver.html?searchHighlight=explicit%20solver&s_tid=doc_srchtitle
13. ***dSPACE TargetLink, Code Generator Options, Influencing the generated, optimized code, V. 1.0, December 2015.
14. ***ControlDesk Next Generation Reference For ControlDesk 5.3, Release 2014-B, November 2014.
15. ***ControlDesk Next Generation Experiment Guide, For ControlDesk 5.3, Release 2014-B, November 2014.